

Multiscale structural topology optimization

Liang Xia, Piotr Breitkopf

Sorbonne universités, Université de technologie de Compiègne, CNRS, Laboratoire Roberval, Centre de Recherches de Royallieu, CS 60319, 60203, Compiègne Cedex, France, liang.xia@utc.fr

1. Abstract

This work develops firstly a nonlinear framework for concurrent topology optimization of material and structure. It has been shown that though linear models are assumed at both scales, the structural equilibrium is in general nonlinear due to the adaptation of local material microstructures. Secondly, the new regime of nonlinearity due to material optimization is approximated by a precomputed database model. As a result of this off-line step, the effective strain-energy and stress-strain relations required for the concurrent design are provided in a numerically explicit manner, which significantly reduces computational cost and enables design of larger-scale problems.

2. Keywords: Model reduction, Homogenization, Multiscale analysis, Topology optimization

3. Introduction

Existing researches of topology optimization focus mainly on monoscale designs, either designing homogeneous structures [1], or designing materials for expected effective performance [2]. A usual strategy applied to bridge the two scales is designing an universal material microstructure either for a fixed [3] or concurrently changed [4] structure at the macroscopic scale. In fact, earlier attempt traces back to [5], where simultaneous optimal designs are performed for both structure and elementwisely varying cellular materials following a decomposed design procedure [6]. Concerning multiscale design, cellular materials are designed in response to the displacement solution at the structural scale while their variations in turn modify the structural constitutive behavior. The equilibrium problem at the structural scale is therefore in general nonlinear. Such nonlinearity has been neglected in the early works (e.g., [4, 5]) where both scale design variables were updated simultaneously and the equilibrium at the structural scale was not enforced.

Unlike the previous models, in [7] we revisited concurrent topology optimization of material and structure while using a nonlinear iterative solution scheme, FE² [8], to address the nonlinearity due to the optimization or the adaptation of material microstructures. In addition, we have defined cellular material models pointwisely that in the context of finite element analysis they were assigned at the Gauss integration points. A schematic illustration of concurrent topological design of material and structure is shown in Fig. 1. Bi-directional Evolutionary Structural Optimization (BESO) method [9] was applied for the designs at both scales. Note that, this concurrent design framework requires intensive computational cost due to large number of repetitive material optimizations.

In our successive work [10], in viewing the material optimization process as a generalized constitutive behavior, we made a step further and adapt the Numerically EXplicit Potentials (NEXP) model [11] to approximated this new regime of nonlinearity. By this model, we constructed firstly a database from a set of numerical experiments so as to describe the effective strain energy density in a test space of macroscopic strain tensor. By tensor decomposition, a continuous representation of the strain energy density function is built as a sum of products of one-dimensional interpolation functions. As a result of this *a priori* off-line step, the effective strain-energy and stress-strain relations required for macroscopic structural evaluation and optimization are provided in a numerically explicit manner. The explicit material behavior representation given by the reduced database model is then used to serve the concurrent design [7] at a negligible computational cost.

4. Multiscale structural topology optimization [7]

Let $\rho(x)$ and $\eta(x, y)$ denote the design variables at the two scales, respectively. \mathcal{A} defines an integral admissible set consisting of two subsets \mathcal{A}_ρ and \mathcal{A}_η for $\rho(x)$ and $\eta(x, y)$, respectively. Both variables take binary values: 0 or 1, indicating void and solid materials, respectively. Volume fraction constraints are considered. Using the principle of minimum potential energy, the minimum compliance problem in a displacement-based formulation is [12]

$$\max_{(\rho, \eta) \in \mathcal{A}} \min_{u \in \mathcal{U}} \left\{ \frac{1}{2} \int_{\Omega} C_{ijkl}(x, \rho, \eta) \frac{\partial u_i}{\partial x_j} \frac{\partial u_k}{\partial x_l} d\Omega - l(u) \right\}, \quad (1)$$

where $C_{ijkl}(x, \rho, \eta)$ is the fourth-order elastic stiffness tensor at point x depending on $\rho(x)$ and $\eta(x, y)$. \mathcal{U} denotes the space of kinematically admissible displacement fields and $l(u)$ is the loading potential term. Since $\rho(x)$ and

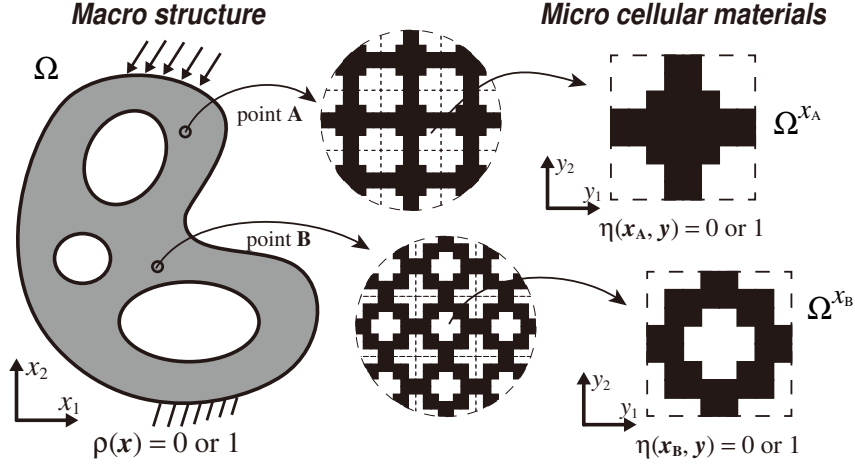


Figure 1: Illustration of concurrent topology optimization of material and structure [7, 10].

$\eta(x, y)$ are defined independently at two scales, Eq. (1) can be reformulated to

$$\max_{\rho \in \mathcal{A}_\rho} \min_{u \in \mathcal{U}} \left\{ \int_{\Omega} \left\{ \max_{\eta \in \mathcal{A}_\eta} \frac{1}{2} C_{ijkl}(x, \rho, \eta) \frac{\partial u_i}{\partial x_j} \frac{\partial u_k}{\partial x_l} \right\} d\Omega - l(u) \right\}, \quad (2)$$

where the pointwise maximization of strain energy density is treated as a subproblem. Note that, because materials defined at the microscopic scale are optimized according to the current strain loading statuses and the optimized materials in turn update the constitutive behavior at the macroscopic scale, the interface equilibrium is therefore in general nonlinear even though linear models are assumed at both scales.

To address this interface nonlinearity, we employ a nonlinear iterative solution scheme, so named FE² according to [8]. In general nonlinear case, it asserts that each point of the macroscopic discretization is associated with a Representative Volume Element (RVE). Then for each macroscopic equilibrium iteration, a nonlinear load increment has to be computed for each of the (many) RVEs. In return the average stress across the RVE is then used as the macroscopic stress tensor without the need of effective constitutive relations at hand. Therefore, the macroscopic stress $\Sigma(x)$ is computed as a function of the microscopic stress state by means of volume averaging (or via surface integrals) according to

$$\Sigma(x) = \langle \sigma(x, y) \rangle = \frac{1}{|\Omega^x|} \int_{\Omega^x} \sigma(x, y) dV = \frac{1}{|\Omega^x|} \int_{\partial\Omega^x} t \otimes x dA. \quad (3)$$

Similarly, the macroscopic strain $E(x)$ defines the mean of the microscopic strain via

$$E(x) = \langle e(x, y) \rangle = \frac{1}{|\Omega^x|} \int_{\Omega^x} e(x, y) dV = \frac{1}{|\Omega^x|} \int_{\partial\Omega^x} \text{sym}(u \otimes n) dA, \quad (4)$$

where n is the normal vector on the boundary of the microstructure. The interface equilibrium is solved iteratively using the Newton-Raphson method

$$\mathcal{R}(u, \rho, \eta) = f_{\text{ext}} - \int_{\Omega} B^T \langle \sigma(x, y) \rangle d\Omega = 0, \quad (5)$$

where $\mathcal{R}(u, \rho, \eta)$ and f_{ext} are the residual and external force at the macroscopic scale, respectively, and B is the linear strain-displacement matrix. It is important to emphasize that $\sigma(x, y)$ is evaluated on the optimized material, which is obtained using the BESO method [9] according to the imposed macroscopic strain $\langle e(x, y) \rangle = E(x)$.

4.1. Material design for a two-scale bridge-type structure

In order to illustrate the equilibrium nonlinearity due to the material optimizations, a simple two-scale bridge-type structure (Fig. 2(a)) is considered, where the cellular materials are optimized so as to maximize the global structural stiffness. The bridge-type structure is discretized into quadratic 8-node elements. Four Gauss integration points are defined for each finite element and each integration point is attributed with a cellular material model discretized into 80×80 bilinear 4-node elements. Young's modulus and Poisson's ratio of solid material at the microscopic scale are set to be 1 and 0.3, respectively. Volume fraction constraint for each cellular material model is set to 60%.

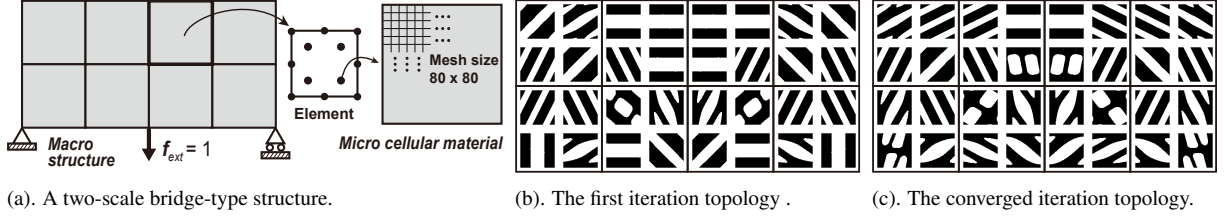


Figure 2: Illustration of the equilibrium nonlinearity: material design for a bridge-type structure [7].

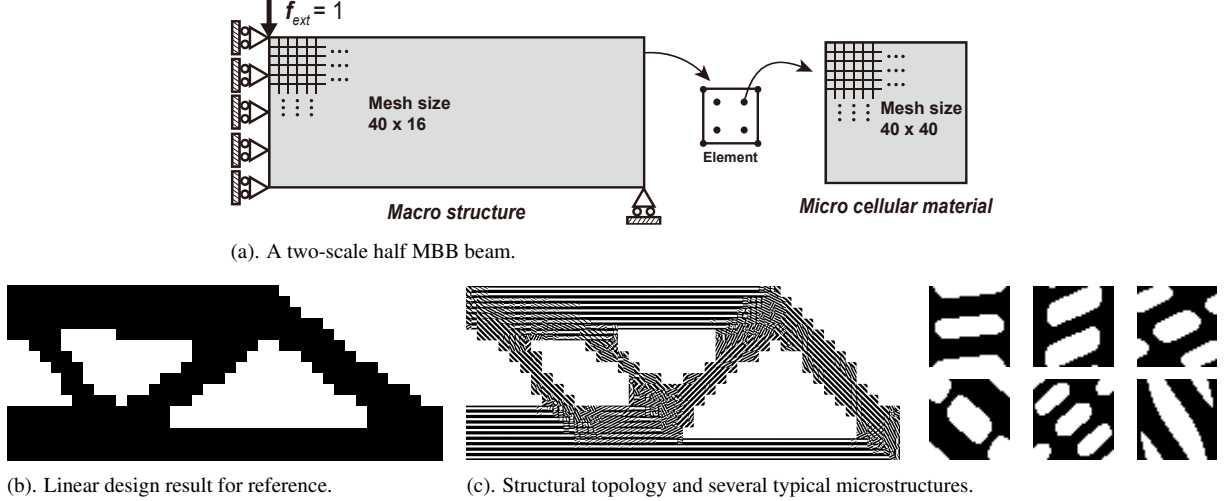


Figure 3: Concurrent topological design of a two-scale half MBB beam [7].

The evolution rate in the BESO is set to 0.02, which determines the percentage of removed material at each design iteration. Sensitivity filtering is used to avoid checkerboard pattern and mesh-dependency.

The topologies of the first and the converged (6th) iterations are shown in Figs. 2(b) and (c), respectively. The difference between Figs. 2(b) and (c) demonstrates the necessity of considering the nonlinearity of the interface equilibrium. Note that, in Figs. 2(b) and (c) the optimized cellular materials on the Gauss points are enlarged for a clear visualization. Upon the homogenization theory, the optimized cellular material only represents the optimal design at the microscopic scale for that material point, i.e., Gauss integration point. Therefore, the optimized cellular materials in the neighboring points represent only the tendency of the topological variations while are not necessarily continuous.

4.2. Concurrent material and structure design for a two-scale MBB beam

In this example, the so-called MBB beam [12] is considered and optimal designs are carried out concurrently at both structural and material scales. Due to the symmetry of the problem, only half MBB beam is considered as shown in Fig. 3(a). The macroscopic structure is discretized into 40×16 bilinear 4-node elements, which means in total $N_{gp} = 4 \times 40 \times 16$, 2560 cellular material models are considered concurrently at the microscopic scale. At the macroscopic structure, $N = 40 \times 16$, 640 design variables are accordingly defined. Microscopic cellular material model is discretized into 40×40 bilinear 4-node elements with $M = 40 \times 40$ design variables. Volume constraints of solid material are set to 60% at both scales. The evolution rate in the BESO is set to 0.02 and sensitivity filtering is applied as in the previous example.

It takes around 6 solution iterations to reach the macroscopic equilibrium for each design iteration. The final topologies of both cellular materials and structure are shown in Fig. 3(c). The standard monoscale design within the regime of linear elasticity is given in Fig. 3(b) for the purpose of comparison. Some typical microstructures obtained in the nonlinear two-scale design is also given in Fig. 3(c). Similarly, the optimized cellular material only represents the optimal design at the microscopic scale for that material point satisfying the assumptions of scale-separation and periodicity. The optimized cellular materials in neighboring points represent only the tendency of the topological variations. As can be observed in Fig. 3(c), uniaxial materials may be sufficient at the main branches of the structure; while in order to have a higher structural performance, anisotropic materials have to be used at the joints of the main branches due to the more complex loading status.

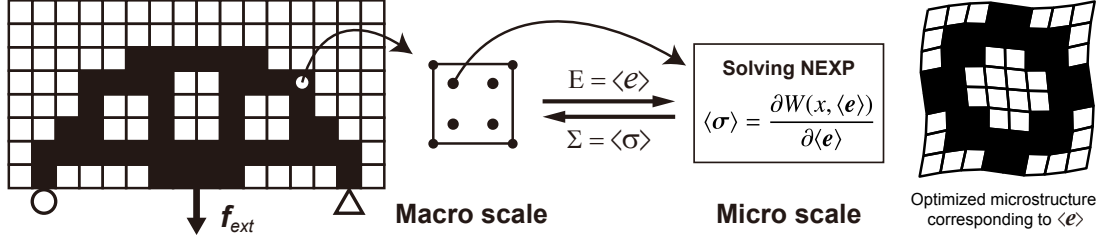


Figure 4: Illustration of the monoscale structural design with the NEXP model [10].

5. Reduced multiscale structural topology optimization [10]

In viewing the local material optimization process as a particular regime of material nonlinearity, the main objective of this part of work is to construct an explicit representation of the strain energy density $W(\langle e \rangle)$ in terms of $\langle e \rangle$ such that the concurrent design can be performed with an effective stress-strain relationship provided at an extremely reduced computational cost. For such reason, following the NEXP strategy [11], we construct an approximate expression of $W(\langle e \rangle)$ using a precomputed database. An illustrative scheme is shown in Fig. 4.

The NEXP model aims to construct an explicit approximation $\tilde{W}(\langle e \rangle)$ over the tensor space using a precomputed database and interpolation schemes, expecting $\tilde{W}(\langle e \rangle)$ close enough to $W(\langle e \rangle)$

$$W(\langle e \rangle) \approx \tilde{W}(\langle e \rangle) = \sum N_q(\langle e \rangle) W_q, \quad (6)$$

where N_q are the interpolation functions and W_q are the strain energy density values stored in the database, which are evaluated by means of a set of numerical experiments over the test tensor space. It is important to emphasize that W_q corresponds to the energy density of an optimized material for a given $\langle e \rangle_q$. Once the database model is built, the effective stress-strain relationship is obtained as

$$\langle \sigma \rangle \approx \sum \frac{\partial N_q(\langle e \rangle)}{\partial \langle e \rangle} W_q, \quad (7)$$

provided the interpolation functions N_q are continuously differentiable.

Still following [11], the precomputed full database is further approximated by a sum of products of one-dimensional interpolation functions via higher-order tensor decomposition. The Voigt notation is applied such that $\{\langle e \rangle_1, \langle e \rangle_2, \langle e \rangle_3, \langle e \rangle_4, \langle e \rangle_5, \langle e \rangle_6\}$ corresponds to $\{\langle e \rangle_{11}, \langle e \rangle_{22}, \langle e \rangle_{33}, \langle e \rangle_{23}, \langle e \rangle_{13}, \langle e \rangle_{12}\}$. Let \mathbb{W} denote the hypermatrix which stores the database. It can be approximated in a tensor decomposed representation

$$\mathbb{W} \approx \sum_{r=1}^R \phi_1^r \otimes \phi_2^r \otimes \cdots \otimes \phi_6^r, \quad (8)$$

where ϕ_j^r are real-valued vectors corresponding to the effective strain tensor components $\langle e \rangle_j$ and R is the number of expanded terms. The vectors ϕ_j^r involved in (8) are determined by solving the following least square problem for a given value of R

$$\inf_{\phi_j^r} \left\| \mathbb{W} - \sum_{r=1}^R \phi_1^r \otimes \phi_2^r \otimes \cdots \otimes \phi_6^r \right\|^2, \quad (9)$$

where $\|\cdot\|$ is the Frobenius norm. Once the decomposed vectors in (8) are obtained, the continuous representation of $W(\langle e \rangle)$ written in terms of separated components can be constructed by interpolation

$$W(\langle e \rangle_1, \langle e \rangle_2, \dots, \langle e \rangle_6) \approx \sum_{r=1}^R \tilde{\phi}_1^r(\langle e \rangle_1) \tilde{\phi}_2^r(\langle e \rangle_2) \cdots \tilde{\phi}_6^r(\langle e \rangle_6), \quad (10)$$

where $\tilde{\phi}_j^r(\langle e \rangle_j)$ are the interpolated values of ϕ_j^r . The tensor decomposed database requires only one-dimensional interpolations for effective stress evaluation, which further reduces computing time.

5.1. Validation of the NEXP model

Consider the same cellular material model setting as in the previous section. The NEXP model is built over the strain domain. Each dimension of the strain space is discretized into $p = 21$ uniformly distributed points, which means in total 21^3 local material optimizations are carried out at the off-line phase. With a relative reconstruction

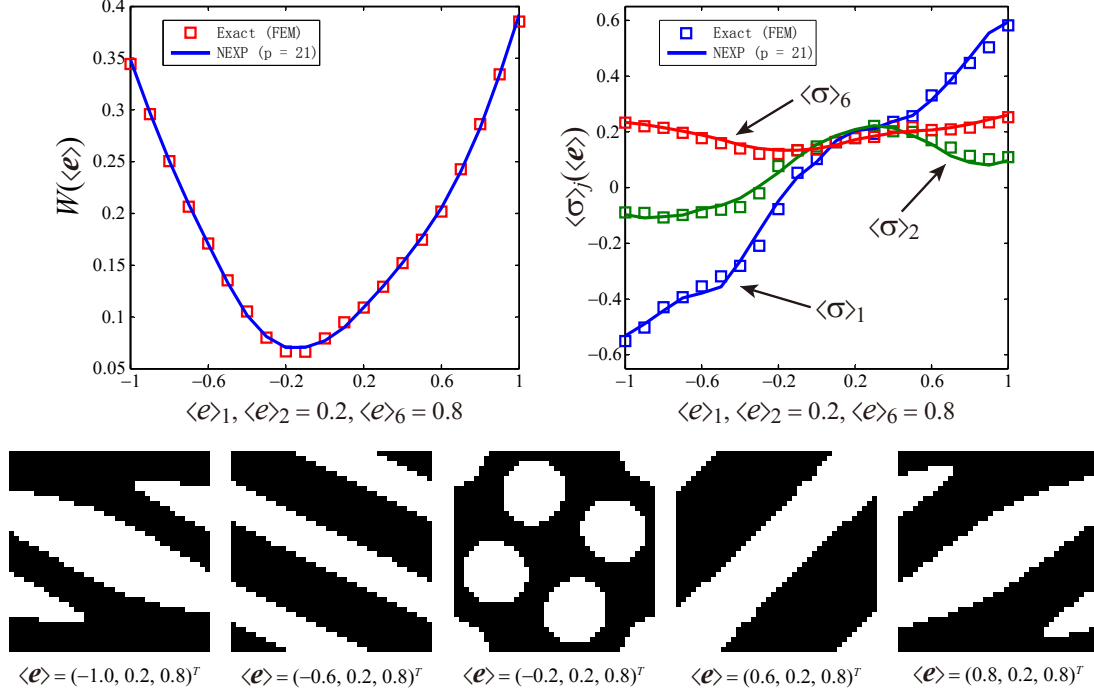


Figure 5: Comparison of the exact and approximate values evaluated using FEM and NEXP [10].

error chosen as 0.01, we obtain $R = 9$ truncated modes in each dimension for the reduced approximation \tilde{W} . To validate the performance, we compare the values evaluated using the NEXP model and the exact computations. A first comparison is given in Fig. 5, where $\langle e \rangle_2 = 0.2$, $\langle e \rangle_6 = 0.8$ are fixed and $\langle e \rangle_1$ varies from -1 to 1 . Several observations can be found from Fig. 5. Firstly, the approximate values given by the NEXP model are in very good agreement with the exact solutions. Secondly, the strain energy density is a convex function over the effective strain space. Thirdly, the selected optimal material microstructures show the tendency of topological variation along $\langle e \rangle_1$, which introduces nonlinearity to the interface equilibrium.

5.2. Design of a two-scale half MBB beam with fine discretization

With the constructed NEXP model, we are now capable of designing a much larger scale or finely discretized two-scale MBB beam with 120×60 bilinear 4-node elements. Volume constraint at the macroscopic structure is set to 60%. The evolution rate in the BESO is set to 0.02 and sensitivity filtering is applied. Fig. 6 gives the optimized structure topology together with the retrieved optimal cellular material topologies. Three local zones are selected and zoomed for a better visualization of microscopic material topologies. This test takes around 6 hours for all 35 design iterations on the used personal computer. Retrieving microscopic material topologies at the final design requires one additional hour computing. Assuming 6 substeps required in average for each structural design iteration and one hour computing for each substep of each design iteration, then the concurrent design strategy [7] would require in total more than 200 hours computing time for solving this problem on the used personal computer. In the contrast, using the constructed NEXP material model, it requires only 7 hours computing to reach the final design. Note that this time can still be further reduced with parallel computing.

6. Conclusion

This work develops a FE^2 -based multiscale structural topology optimization framework and adapts the NEXP strategy into this framework to limit the computational cost. This framework is independent with the type of design variables, other parameters such as geometrical or even manufacturing process parameters can be considered for the design. Future works will focus on considering more realistic multiscale structures constituted by 3D knitted or woven composites with more complex nonlinear constitutive behaviors.

7. Acknowledgements

This work was carried out in the framework of the Labex MS2T, which was funded by the French Government, through the program “Investments for the future” managed by the National Agency for Research (Reference ANR-11-IDEX-0004-02).

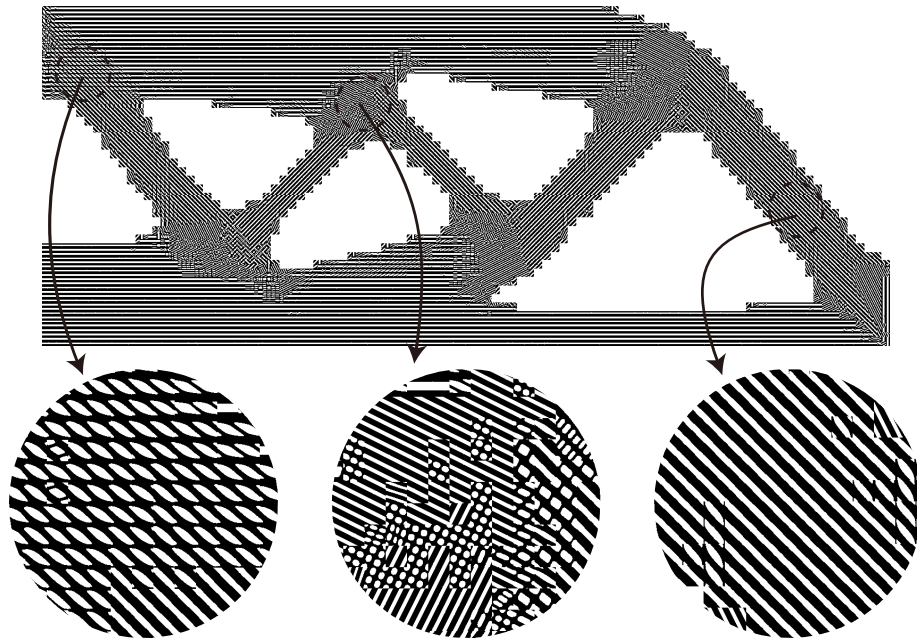


Figure 6: Two-scale design of half MBB beam with retrieved local optimal material topologies [10].

8. References

- [1] J.D. Deaton, R.V. Grandhi, A survey of structural and multidisciplinary continuum topology optimization: post 2000, *Structural and Multidisciplinary Optimization*, 49, 1-38, 2014.
- [2] J. Cadman, S. Zhou, Y. Chen, Q. Li, On design of multi-functional microstructural materials, *Journal of Materials Science*, 48, 51-66, 2013.
- [3] X. Huang, S. Zhou, Y.M. Xie, Q. Li, Topology optimization of microstructures of cellular materials and composites for macrostructures. *Computational Materials Science*, 67, 397-407, 2013.
- [4] X. Yan, X. Huang, Y. Zha, Y.M. Xie, Concurrent topology optimization of structures and their composite microstructures, *Computers and Structures*, 133, 103-110, 2014.
- [5] H. Rodrigues, J.M. Guedes, M.P. Bendsøe, Hierarchical optimization of material and structure, *Structural and Multidisciplinary Optimization*, 24(1):1-10, 2002.
- [6] M.P. Bendsøe, A.R. Diaz, R. Lipton, J.E. Taylor, Optimal design of material properties and material distribution for multiple loading conditions, *International Journal for Numerical Methods in Engineering*, 38(7):1149-1170, 1995.
- [7] L. Xia, P. Breitkopf, Concurrent topology optimization design of material and structure within FE^2 nonlinear multiscale analysis framework, *Computer Methods in Applied Mechanics and Engineering*, 278, 524-542, 2014.
- [8] F. Feyel, J. Chaboche, FE^2 multiscale approach for modelling the elastoviscoplastic behaviour of long fibre sic/ti composite materials, *Computer Methods in Applied Mechanics and Engineering*, 183, 309-330, 2000.
- [9] X. Huang, Y. M. Xie, *Topology Optimization of Continuum Structures: Methods and Applications*, John Wiley & Sons, Chichester, 2010.
- [10] L. Xia, P. Breitkopf, Multiscale structural topology optimization with an approximate constitutive model for local material microstructure, *Computer Methods in Applied Mechanics and Engineering*, 286, 147-167, 2015.
- [11] J. Yvonnet, D. Gonzalez, Q. C. He, Numerically explicit potentials for the homogenization of nonlinear elastic heterogeneous materials, *Computer Methods in Applied Mechanics and Engineering*, 198, 2723-2737, 2009.
- [12] M. P. Bendsøe, O. Sigmund, *Topology optimization: theory, methods and applications*, Springer-Verlag, Berlin, 2003.